VR_cI_c Photometric Study of the Totally Eclipsing Pre-W UMa Binary, V616 Camelopardalis: Is it Detached?

Ronald G. Samec
Faculty Research Associate, Pisgah Astronomical Research Institute, 1 PARI Drive, Rosman, NC 28772; ronaldsamec@gmail.com

Daniel B. Caton
Davis R. Gentry
Dark Sky Observatory, Department of Physics and Astronomy, Appalachian State University, 525 Rivers Street, Boone, NC 28608-2106; catondb@appstate.edu, gentrydr@appstate.edu

Danny R. Faulkner
Johnson Observatory, 1414 Bur Oak Court, Hebron, KY 41048

Received May 16, 2019; revised July 8, 26, August 9, 2019; accepted August 16, 2019

Abstract V616 Cam is a F3V±3 type (T ~ 6750 ± 400 K) eclipsing binary. It was observed on March 5, 6, 9, and 30, 2017, at Dark Sky Observatory in North Carolina with the 0.81-m reflector of Appalachian State University. Five times of minimum light were determined from our present observations, which include three primary eclipses and two secondary eclipses. In addition, two other timings were given, one in VSX, and one in Shaw's list of near contact binaries. The following quadratic ephemeris was determined from the available times of minimum light: JD Hel Min I = 2457817.8367 ± 0.0016 d + (0.52835050 ± 0.00000108) × E – (0.00000000238 ± 0.000000000009) × E^2. The rapid period decrease may indicate that the binary is undergoing magnetic braking and is approaching its contact configuration. The possibility of a third body is discussed, but no third light was determined in the solution. VR_cI_c simultaneous Wilson-Devinney program solutions preferred a near semi-detached solution (the primary component near filling its critical lobe and the secondary slightly underfilling, ~V1010 Oph type). Mode 2, 4, and 5 solutions were determined to arrive at this result. The noted solution gives slightly better sum of square residuals. This solution gives a mass ratio of ~0.36 and a component temperature difference of ~2090 K. A BINARYMAKER-fitted dark spot altered slightly but was not eliminated in the WD synthetic light curve computations. A 16 ± 2° radius spot is on the larger component above the equator with a T-factor of 0.95. A total eclipse of 38 minutes occurs at phase 0.5.

1. Introduction

In the course of our studies of solar type binaries we have discovered a number of pre-contact systems (Samec *et al.* 2017) on their way to becoming W UMa contact systems. We have designated them as pre-contact W UMa binaries since their orbital period studies have shown them to be systems that are likely undergoing magnetic braking (angular momentum loss, AML). This could lead them to contact and ultimately to coalescence and to the formation of fast rotating earlier spectral type single star following a red novae event (Tylenda and Kamiński 2016). Streaming plasmas moving on stiff, rotating radial patterns away from the binary out to the Alfvén radius (~50 stellar radii) cause this phenomena. Here we present the first precision photometry and light curve analysis of another such candidate, the near-contact system V616 Cam. The first report of these observations was given as a poster paper at the American Astronomical Society Meeting #233 (Samec *et al.* 2019).

2. History

The light curve of NSVS 103152 (V616 Cam) was listed in the near contact binaries list of Shaw and Hou (2007). This list gives the position, magnitude (V = 13.3934), and the ephemeris:

$$\text{JD Hel MinI} = 2451419.956\text{ d} + 0.52839\text{d} \times \text{E}. \quad (1)$$

Figure 1 displays Shaw's light curve.

The AAVSO International Variable Star Index (VSX; Watson *et al.* 2006–2014) gives r = 13.393—? magnitude and an ephemeris of:

$$\text{HJD} = 2440419.95624\text{ d} + 0.52838555 \times \text{E}. \quad (2)$$

The Two Micron All Sky Survey (2MASS; Skrutskie *et al.* 2006) gives a J–K of 0.220 ± 0.044 mag and the AAVSO Photometric All-Sky Survey, data release 9 (APASS-DR9; Henden *et al.* 2015) gives a B–V = 0.32. Hoffman *et al.* (2008) and VSX give epoch T_{min} = 2401536.696006, and a maximum V = 13.29 (catalogue data), and list it as a W UMa binary.

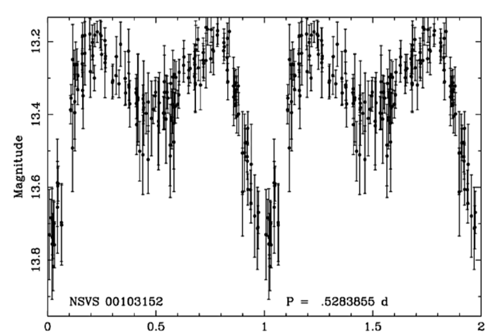

Figure 1. Light curve of V616 Cam (Shaw 1990, 1994; http://www.physast.uga.edu/~jss/ncb/LC/lc10421183.pdf).

This system was observed as a part of our student/professional collaborative studies of interacting binaries using data taken from Dark Sky Observatory (DSO) observations. The observations were taken by R. Samec, D. Caton, and D. Faulkner. Reduction and analyses were done by R. Samec. The GAIA DR2 determined distance is 1211 ± 23 pc (Bailer-Jones 2015). The light curve shown (Figure 2) is available in the ASAS-SN (All-Sky Automated Survey for Supernovae, https://asas-sn.osu.edu/) Variable Stars Data Base (The ASAS-SN Catalog of Variable Stars: II, Shappee *et al.* 2014 and Kochanek *et al.* 2017) with a J–K = 0.22, an ephemeris:

$$\text{JD Hel Min I} = 2457757.06327\,\text{d} + 0.5283593 \times \text{E}, \quad (3)$$

and catalog name: ASASSN-V J090553.27+820344.9. They also give a B–V = 0.322 and an E(B–V) of 0.028, making the corrected B–V ~ 0.294.

3. 2017 VR_cI_c photometry

The observations were taken with the Dark Sky Observatory (DSO) 0.81-m reflector at Philips Gap, North Carolina, on 5, 6, 9, and 30 March 2017 with a thermoelectrically cooled (–35° C) 2K × 2K Apogee Alta camera and Johnson-Cousins VR_cI_c filters. The Individual observations included 280 in V, 287 in R_c, and 285 in I_c. The standard error of a single observation was 10 mmag V, 16 mmag in R_c, and 13 mmag in I_c. The nightly check-comparison star (C–K) values stayed constant throughout the observing run with a precision of 1%. Exposure times varied from 25s in V to 15s in R_c and I_c. Two sample sets of observations from March 5 and 6 are given as Figures 3 and 4. The coordinates and magnitudes of the variable star, comparison star, and check star are given in Table 1.

The finder chart is given as Figure 5 with the variable star (V), comparison star (C), and check star (K) shown. Our observations are listed in Table 2, with magnitude differences ΔV, ΔR_c, and ΔI_c in the sense variable minus comparison star.

4. Orbital period study

Five times of minimum light were calculated, three primary and two secondary eclipses, from our present observations. Two times of minimum light are listed in the literature (Hubscher and Lehmann 2012). VSX also gives a time of minimum light.

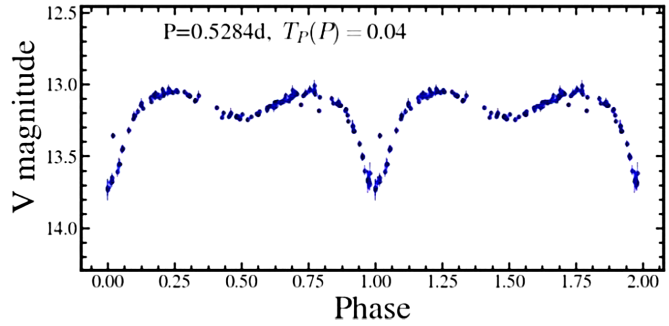

Figure 2. V light curve of V616 Cam (ASASSN-V J090553.27+820344.9) (https://asas-sn.osu.edu/).

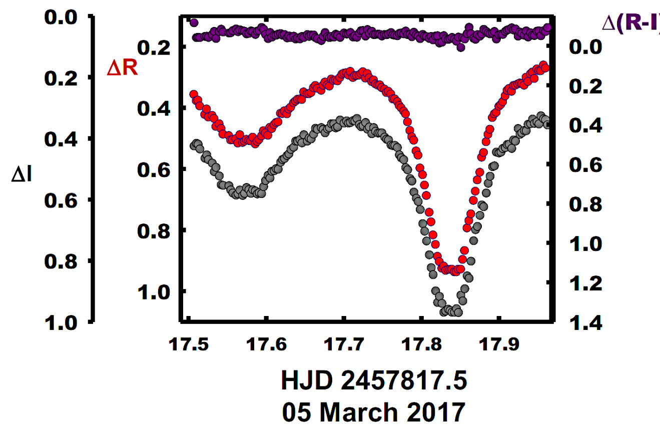

Figure 3. R_c, I_c, and R_c–I_c color curves on the night of 5 May 2017.

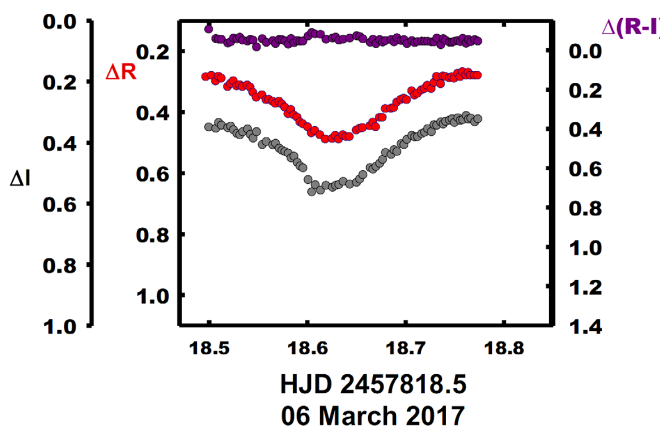

Figure 4. R_c, I_c, and R_c–I_c color curves on the night of 6 March 2017.

Table 1. Photometric targets.

Star		*Name*[1]	*R.A. (2000)* *h m s*	*Dec. (2000)* *° ′ ″*	*V*[1]	*J–K*[2]
Variable	V	V616 Cam GSC 4547 0771 3UC345-013290	09 05 52.600	+82 03 44.4	13.19	0.22 ± 0.02
Comparison	C	GSC 4547 0773 3UC345-013321	09 07 26.9480	+82 03 48.200	12.92	0.260 ± 0.035
Check	K	GSC4547 1067 3UC345-013313	09 06 57.1873	+82 00 28.91	13.34	0.420 ± 0.046

[1] *UCAC3 (U.S. Naval Obs. 2012).* [2] *2MASS (Skrutskie et al. 2006)*

Shaw and Hou's (2007) list of near contact binaries gives an ephemeris. All of these times of minimum light are given in Table 3. Linear and quadratic ephemerides were determined from these data:

$$\text{JD Hel Min I} = 2457817.8526 \text{ d} + 0.5283783 \quad \pm 0.0127 \quad \pm 0.0000025 \tag{4}$$

$$\text{JD Hel Min I} = 2457817.8367 \text{ d} + 0.52835050 \times E - 0.00000000238 \times E^2 \quad \pm 0.0016 \quad \pm 0.00000108 \quad \pm 0.00000000009. \tag{5}$$

The period study covers a time interval of some 17.5 years and shows a period that is decreasing (at a high precision level; the errors shown here are standard errors). The rapid period decrease may indicate that the binary is undergoing magnetic braking and is approaching its contact configuration. The main problem at this point is the small number of times of minimum light. However, the first "minima" in Table 3 is an epoch from a period study, the second "point" is actually two data points (Hubscher and Lehmann 2012), and the last "one" is actually five minima. The quadratic ephemeris yields a $\dot{P} = -3.304 \pm 0.014 \times 10^{-6}$ d/yr or a mass exchange rate of

$$\frac{dM}{dt} = \frac{\dot{P} M_1 M_2}{3P\,(M_1 - M_2)} = \frac{1.62 \pm 0.54 \times 10^{-6}\ M_\odot}{\text{d}} \tag{6}$$

in a conservative scenario. Since the possibility of a third component must be considered, the apparent quadratic curve could be part of a sinusoid. In fact, a large percentage of short-period systems have third components (Tokovinin *et al.* 2006). Further eclipse timings are needed to confirm or disaffirm this scenario.

A plot of the quadratic residuals is given in Figure 6. The quadratic fit carried a precision of 27 sigma. Again, this result should not be taken with high credibility due to the relatively small number of data points. The O–C quadratic residual calculations are given in Table 3.

If the resulting trend is continuous, ultimately the system would become unstable, resulting in a red novae event, and finally coalesce into a single fast rotating spectrally, earlier star (Tylenda and Kamiński 2016). Alternately, the period change could a part of a sinusoidal variation due to the presence of a third body.

5. Light curves

The VR_cI_c phased light curves calculated from Equation 2 are displayed in Figures 7a and 7b. The light curve averages at quarter phases and characteristics are given in Table 4. The amplitude of the light curve varies from 0.69 to 0.64 mag in V to I_c. The O'Connell effect, as a possible indicator of spot activity (O'Connell 1951; i.e., Guinan *et al.* 1991), is appreciable, averaging 0.06 mag. The differences in minima are large, 0.41–0.46 mag from I_c to V, probably indicating noncontact light curves. The amplitudes of the light curves are 0.64 to 0.69 mag, I_c to V, indicating a fairly large inclination for near contact curves. The $V–I_c$ and $R–I_c$ color curves fall at phase 0.0, which is characteristic of a contact binary, however the color curves

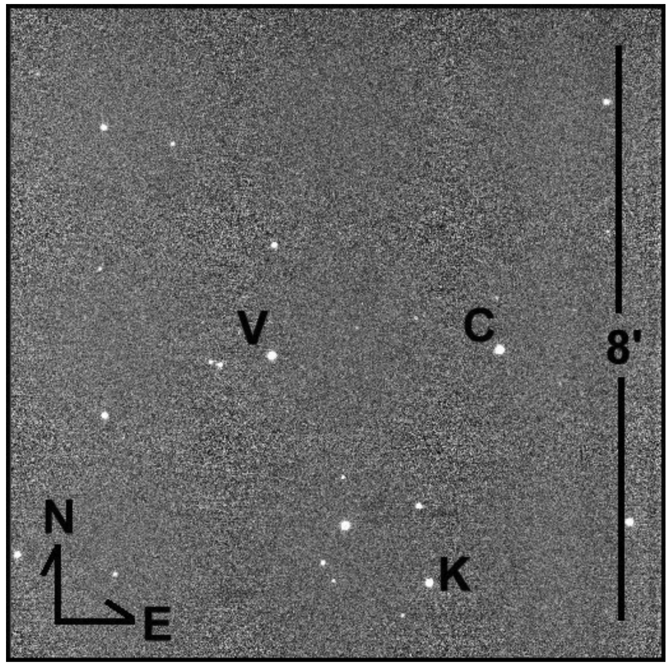

Figure 5. Finder chart: V616 Cam (V), comparison star (C), and check star (K).

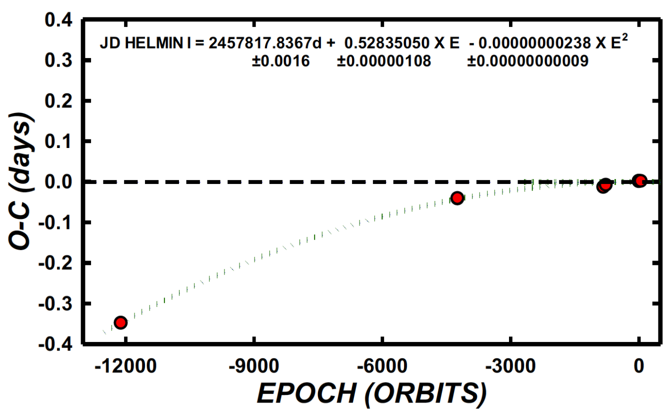

Figure 6. The period study of 17.5 years indicates continuous period decrease for V616 Cam.

rise slightly at phase 0.5, which indicates that the secondary component is under filling its Roche Lobe. Thus, the shape of the curves indicates a near-semidetached binary coming into contact.

6. Temperature

2MASS gives a J–K = 0.22 for the binary. The APASS-DR9 gives B–V = 0.32 (E(B–V) given earlier). These correspond to a F3V±3 eclipsing binary (Mamajek 2019). This yields a temperature of 6750 ± 400 K. Fast rotating binary stars of this type are known for having convective atmospheres, so spots are expected and indeed, one major spot is found.

We have modeled a number of short period F-type binaries with magnetic spot activity. These include V500 Peg (Caton *et al.* 2017), FF Vul (Samec *et al.* 2016a), V500 And (Samec *et al.* 2016b), and GSC 3208 1986 (Samec *et al.* 2015), to name a few.

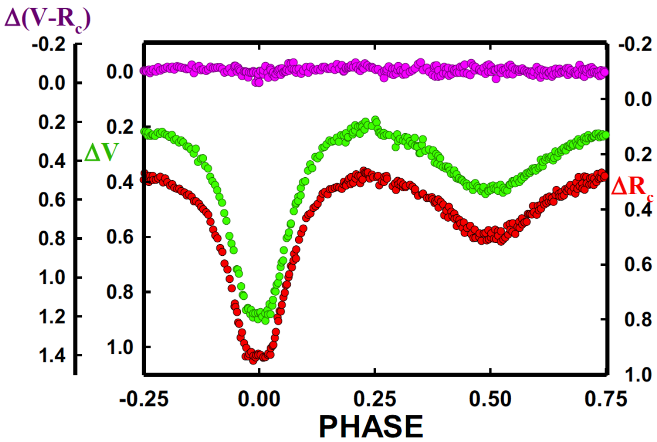

Figure 7a. V, R_c light curves and V–R color curves (Variable-Comparison), magnitudes phased with Equation 2.

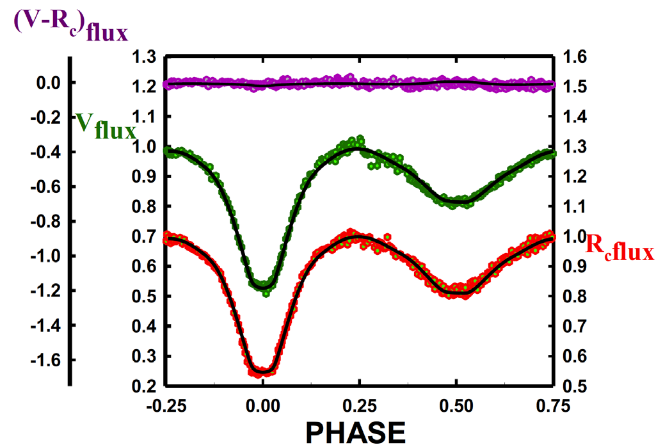

Figure 8a. V, R_c normalized fluxes and the V–R color curves overlaid by the detached solution for V616 Cam.

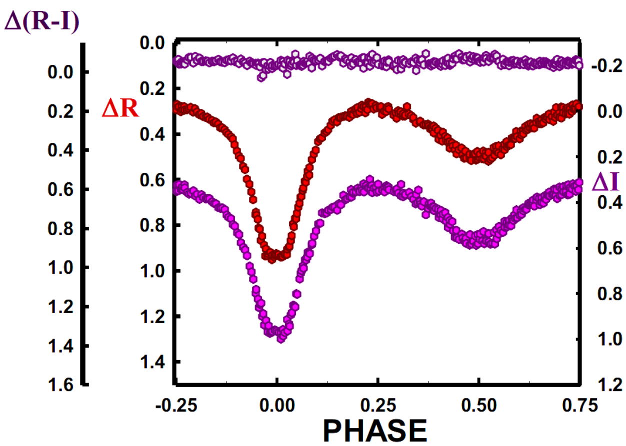

Figure 7b. R_c,I_c light curves and R_c–I_c color curves (Variable-Comparison), magnitudes phased with Equation 2.

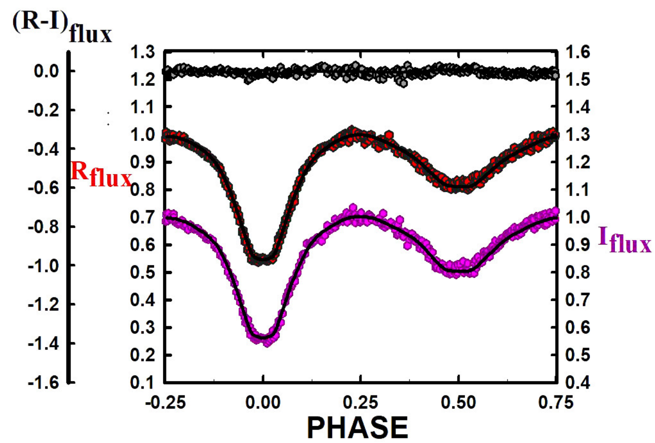

Figure 8b. R_c, I_c normalized fluxes and the R–I color curves overlaid by the detached solution of NSV 103152.

7. Light curve solution

The V, R_c, and I_c curves were pre-modeled with BINARY MAKER 3.0 (Bradstreet and Steelman 2002, but uses black body atmospheres) and fits were determined in the three filter bands. The result of the average best fit is that of a critical contact eclipsing binary with a fill-out of 100.5%. The fill-out of a contact binary is

$$F = \frac{(\Omega_1 - \Omega_{ph})}{(\Omega_1 - \Omega_2)}, \tag{7}$$

where the photometric potential, Ω_{ph}, is between the inner critical potential, Ω_1, and the outer Ω_2, $\Omega_2 \leq \Omega_{ph} \leq \Omega_1$. Other results included q (mass ratio) = 0.37, inclination (i) = 86°, and $\Delta T = 1918$ K. The fill-out would indicate in themselves that the Roche lobes of both components were near or slightly over contact. However, the large difference in component temperatures would show that the components are not in contact. The parameters were then averaged and input into a three-color simultaneous light curve calculation using the WILSON-DEVINNEY program (WD; Wilson and Devinney 1971; Wilson 1990, 1994; Van Hamme 1998). Convective parameters g = 0.32, A = 0.5 were used. Third light was tried and it gave nonphysical (negative) values. The solution was started in Mode 2 to allow the computation itself to determine the actual configuration. The curves converged to a solution in the detached mode, however, the primary component fill-out was 99.99%. The secondary was under-filling at 99.8%. We define the fill-out for a semi-detached or detached binary as simply the critical surface potential, (Ω_1), divided by the actual surface potential, (Ω_{ph}), and it may be expressed in percentages. A Mode 4 solution was computed (with the primary component critically filling its Roche lobe, and the secondary under-filling, the V1010 Oph (Shaw 1994) type binary configuration). The V1010 Oph type binary is the first contact phase of the near contact binary, i.e., the more massive binary is the first to fill its Roche lobe. The solution was completed and the sum of square residuals were very similar with the detached one but slightly worse. The fill-out of the secondary component was 99.5%. Thus, the binary is very near this configuration and very near contact. The difference in the component temperatures, some 2090 K, precludes contact. Additionally, as suggested by the referee, a Mode 5 (Algol, secondary component filling its critical lobe and the primary star underfilling) solution was run. Again, the sum of square residuals for the detached solution was slightly better than either the V1010 Oph (Mode 4) or the Algol (Mode 5). The solutions follow in Tables 5a and 5b. The normalized V and the

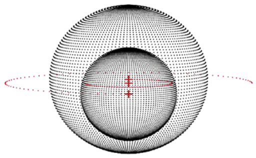

Figure 9a. V616 Cam, geometrical representation at phase 0.00.

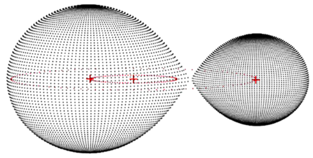

Figure 9b. V616 Cam, geometrical representation at phase 0.25.

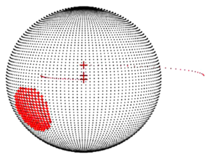

Figure 9c. V616 Cam, geometrical representation at phase 0.50.

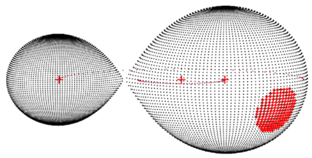

Figure 9d. V616 Cam, geometrical representation at phase 0.75.

R_c,I_c light curves with the detached solution curves overlain are displayed in Figures 8a and 8b. The Roche lobe surfaces are given in Figures 9a–9d. The limb darkening coefficients are two dimensional coefficients logarithmic (x and y) provided in the WD program (Wilson 1990).

8. Discussion

V616 Cam is apparently between a precontact and critical contact W UMa binary configuration with the primary component very near or at its critical contact. This configuration can result when a binary is first evolving into contact. Its spectral type indicates a surface temperature of ~6750 K for the primary component. The secondary component has a temperature of ~4657 K (K3.5V), which means that it is under-massive as compared to a single main sequence star ($M_1 = 1.4\,M_\odot$, $M_2 = 0.73\,M_\odot$). The mass ratio is ~0.36 rather than the expected 0.52. This would be expected for a system undergoing magnetic decay or where the primary component is receiving mass from the secondary and the mass ratio is becoming more extreme. The fill-out of both components is between 99% and critical contact by potential with the primary nearer one. The inclination is 85.7°, which causes a total eclipse of 38 minutes to occur at phase 0.5. The primary component has an iterated cool spot region of 16 ± 2° with a mean T-factor of ~0.95 (T ~ 6410 K). This was not unexpected for solar type binaries. Again, there is certainly a possibility of a third component. However, no third light was determined in the solutions. The apparent quadratic curve could be part of a sinusoid. Further eclipse timings are needed to confirm or disaffirm this scenario.

9. Conclusion

The period study of this pre-contact W UMa binary has a 17.5-year time duration. The period is found to be strongly decreasing at a high level of significance. This is expected for a massive solar type binary undergoing magnetic braking. The presence of a cool magnetic spot would confirm this scenario. If this is indeed the case, the system will slowly coalesce over time as it loses angular momentum due to ion winds moving radially outward on stiff magnetic field lines rotating with the binary (out to the Alfvén radius). If it is not already in contact, the system will soon become a W UMa contact binary and, ultimately, one would expect the binary to become a rather normal, fast rotating, single A2V type field star after a red novae coalescence event (with a ~5% mass loss, Tylenda and Kamiński 2016). Finally, radial velocity curves are needed to obtain absolute (not relative) system parameters.

10. Acknowledgements

Dr. Samec wishes to thank Appalachian State University for allowing us use of the DSO 32-inch F/8 R-C reflector for our many projects.

References

Bailer-Jones, C. A. L. 2015, *Publ. Astron. Soc. Pacific*, **127**, 994.

Bradstreet, D. H., and Steelman, D. P. 2002, *Bull. Amer. Astron. Soc.*, 34, 1224.

Caton, D. B., Samec, R. G., Robb, R., Faulkner, D. R., Van Hamme, W., Clark, J. D., and Shebs, T. 2017, *Publ. Astron. Soc. Pacific*, **129**, 064202.

Guinan, E. F., Bradstreet, D. H., Etzel, P. B., Ibanoglu, C., Ready, C. J., Steelman, D. P., and Thrash, T. A. 1991, *Bull Amer. Astron. Soc.*, **23**, 1412.

Henden, A. A., *et al.* 2015, AAVSO Photometric All-Sky Survey, data release 9 (http://www.aavso.org/apass).

Hoffman D. I., Harrison T. E., Coughlin J. L., McNamara B. J., Holtzman J. A., Taylor G. E., and Vestrand W. T. 2008, *Astron. J.*, **136**, 1067.

Hubscher, J., and Lehmann, P. B. 2012, *Inf. Bull. Var. Stars*, No. 6026, 1.

Kochanek, C. S., *et al.* 2017, *Publ. Astron. Soc. Pacific*, **129**, 104502.

Mamajek, E. 2019, "A Modern Mean Dwarf Stellar Color and Effective Temperature Sequence" Version 2019.3.22 (http://www.pas.rochester.edu/~emamajek/EEM_dwarf_UBVIJHK_colors_Teff.txt).

O'Connell, D. H. K. 1951, *Publ. Riverside Coll. Obs.*, **2**, 85.

Samec, R. G., Caton, D., and Faulkner, D. R. 2019, AAS Meeting #233, id.348.02.

Samec, R. G., Chamberlain, H., Caton, D. B., Faulkner, D. R., Clark, J. D., and Shebs, T. 2016a, *J. Amer. Assoc. Var. Star Obs.*, **44**, 108.

Samec, R. G., Kring, J. D., Robb, R., Van Hamme, W., and Faulkner, D. R. 2015, *Astron. J.*, **149**, 90.

Samec, R. G., Nyaude, R., Caton, D., and van Hamme, W. 2016b, *Astron. J.*, **152**, 199.

Samec, R. G., Olsen, A., Caton, D., and Faulkner, D. R. 2017. *J. Amer. Assoc. Var. Star Obs.*, **45**, 148.

Shappee, B. J., *et al.* 2014, *Astrophys. J.*, **788**, 48.

Shaw, J. S. 1990, in *Proceedings of the NATO Advanced Study Institute on Active Close Binaries*, ed., C. Ibanoglu, Kluwer, Dordrecht, 241.

Shaw, J. S. 1994, *Mem. Soc. Astron. Ital.*, **65**, 95.

Shaw, J. S., and Hou, D. 2007, "Near-Contact Binaries of the Northern Sky Variability Survey" (http://www.physast.uga.edu/~jss/ncb/).

Skrutskie, M. F., *et al.* 2006, *Astron. J.*, **131**, 1163.

Tokovinin, A., Thomas, S., Sterzik, M., and Udry, S. 2006, *Astron. Astrophys.*, **450**, 681.

Tylenda, R., and Kamiński, T. 2016, *Astron. Astrophys.*, **592A**, 134.

U.S. Naval Observatory. 2012, UCAC-3 (http://www.usno.navy.mil/USNO/astrometry/optical-IR-prod/ucac).

Van Hamme, W. V., and Wilson, R. E. 1998, *Bull. Amer. Astron. Soc.*, **30**, 1402.

Watson, C., Henden, A. A., and Price, C. A. 2006–2014, AAVSO International Variable Star Index VSX (Watson+, 2006–2014; http://www.aavso.org/vsx).

Wilson, R. E. 1990, *Astrophys. J.*, **356**, 613.

Wilson, R. E. 1994, *Publ. Astron. Soc. Pacific*, **106**, 921.

Wilson, R. E., and Devinney, E. J. 1971, *Astrophys. J.*, **166**, 605.

Wozniak, P. R., *et al.* 2004, *Astron. J.*, **127**, 2436.

Table 2. V616 Cam observations, ΔV, ΔR_c, and ΔI_c, variable star minus comparison star.

ΔV	*HJD 2457800+*	*ΔV*	*HJD 2457800+*	*ΔV*	*HJD 2457800+*	*ΔV*	*HJD 2457800+*	*ΔV*	*HJD 2457800+*
0.287	17.5086	0.259	17.678	0.879	17.831	0.246	18.527	0.247	18.731
0.300	17.5121	0.240	17.681	0.879	17.834	0.252	18.531	0.253	18.734
0.307	17.5144	0.243	17.684	0.878	17.837	0.256	18.534	0.248	18.738
0.316	17.5166	0.243	17.686	0.878	17.839	0.271	18.537	0.254	18.740
0.345	17.5232	0.243	17.689	0.891	17.842	0.263	18.542	0.232	18.743
0.348	17.5254	0.238	17.692	0.879	17.845	0.271	18.544	0.242	18.747
0.361	17.5276	0.228	17.694	0.867	17.848	0.275	18.547	0.236	18.749
0.360	17.5327	0.226	17.698	0.845	17.850	0.297	18.551	0.227	18.752
0.388	17.5352	0.235	17.700	0.851	17.853	0.247	18.554	0.240	18.755
0.392	17.5377	0.229	17.702	0.798	17.856	0.289	18.557	0.237	18.758
0.397	17.5418	0.231	17.706	0.775	17.858	0.284	18.561	0.237	18.760
0.404	17.5443	0.224	17.708	0.745	17.861	0.308	18.564	0.219	18.764
0.408	17.5468	0.234	17.711	0.694	17.864	0.332	18.567	0.220	18.766
0.413	17.5542	0.235	17.714	0.650	17.866	0.336	18.570	0.222	18.768
0.406	17.5567	0.230	17.717	0.606	17.870	0.342	18.574	0.231	18.773
0.418	17.5592	0.235	17.719	0.585	17.872	0.349	18.577	0.720	21.513
0.435	17.5635	0.222	17.722	0.553	17.874	0.353	18.580	0.812	21.518
0.430	17.5659	0.227	17.725	0.508	17.878	0.347	18.583	0.859	21.524
0.446	17.5684	0.220	17.727	0.477	17.880	0.372	18.586	0.882	21.527
0.435	17.5720	0.229	17.730	0.456	17.883	0.372	18.589	0.894	21.530
0.418	17.5745	0.232	17.733	0.424	17.886	0.374	18.592	0.900	21.536
0.415	17.5770	0.238	17.735	0.403	17.888	0.388	18.595	0.874	21.539
0.428	17.5801	0.231	17.738	0.399	17.891	0.393	18.598	0.906	21.544
0.434	17.5826	0.250	17.741	0.361	17.894	0.418	18.604	0.883	21.547
0.441	17.5883	0.246	17.743	0.338	17.896	0.416	18.607	0.882	21.550
0.430	17.5908	0.259	17.746	0.352	17.899	0.431	18.611	0.830	21.553
0.433	17.5933	0.251	17.749	0.311	17.902	0.424	18.618	0.800	21.556
0.412	17.5965	0.258	17.751	0.316	17.905	0.420	18.623	0.768	21.559
0.399	17.5990	0.273	17.755	0.306	17.907	0.433	18.628	0.711	21.562
0.398	17.6014	0.274	17.757	0.275	17.913	0.431	18.631	0.687	21.564
0.391	17.6046	0.284	17.760	0.265	17.915	0.426	18.635	0.599	21.570
0.402	17.6071	0.299	17.763	0.251	17.919	0.417	18.639	0.556	21.573
0.393	17.6096	0.281	17.766	0.256	17.921	0.412	18.642	0.483	21.579
0.384	17.6127	0.329	17.768	0.253	17.924	0.423	18.646	0.471	21.582
0.376	17.6152	0.317	17.771	0.241	17.927	0.412	18.653	0.451	21.585
0.367	17.6176	0.316	17.774	0.256	17.929	0.406	18.656	0.259	21.636
0.362	17.6209	0.344	17.776	0.232	17.932	0.407	18.659	0.242	21.639
0.358	17.6234	0.353	17.780	0.233	17.935	0.381	18.666	0.230	21.644
0.361	17.6258	0.383	17.782	0.225	17.937	0.381	18.669	0.215	21.647
0.352	17.6291	0.399	17.785	0.239	17.940	0.370	18.672	0.227	21.652
0.321	17.6316	0.413	17.788	0.208	17.943	0.369	18.676	0.193	21.655
0.329	17.6341	0.432	17.790	0.222	17.945	0.353	18.679	0.212	21.658
0.313	17.6378	0.456	17.793	0.196	17.948	0.352	18.682	0.199	21.666
0.313	17.6403	0.477	17.796	0.201	17.951	0.346	18.688	0.186	21.671
0.314	17.6427	0.515	17.798	0.199	17.954	0.345	18.691	0.223	21.674
0.324	17.6458	0.543	17.801	0.201	17.956	0.323	18.694	0.232	21.677
0.291	17.6482	0.598	17.804	0.183	17.960	0.319	18.698	0.224	21.679
0.310	17.6507	0.626	17.806	0.196	17.962	0.308	18.701	0.254	21.696
0.285	17.6552	0.650	17.809	0.176	18.499	0.315	18.704	0.239	21.704
0.282	17.6577	0.719	17.812	0.210	18.502	0.296	18.709	0.241	21.707
0.288	17.6602	0.735	17.815	0.223	18.505	0.293	18.712	0.254	21.709
0.273	17.6633	0.781	17.817	0.235	18.509	0.278	18.715	0.263	21.712
0.263	17.6658	0.816	17.821	0.230	18.512	0.272	18.719	0.242	21.715
0.267	17.6683	0.867	17.823	0.232	18.515	0.275	18.722	0.271	21.718
0.267	17.6732	0.862	17.826	0.238	18.522	0.272	18.725	0.298	21.720
0.271	17.6757	0.866	17.829	0.229	18.524	0.256	18.729	0.267	21.723

Table continued on following pages

Table 2. V616 Cam observations, ΔV, ΔR_c, and ΔI_c, variable star minus comparison star, cont.

ΔR	*HJD 2457800+*	*ΔR*	*HJD 2457800+*	*ΔR*	*HJD 2457800+*	*ΔR*	*HJD 2457800+*	*ΔR*	*HJD 2457800+*
0.357	17.507	0.317	17.676	0.933	17.832	0.315	18.528	0.282	18.738
0.378	17.510	0.326	17.679	0.930	17.835	0.311	18.531	0.284	18.741
0.376	17.512	0.330	17.682	0.930	17.837	0.317	18.534	0.289	18.745
0.395	17.515	0.307	17.684	0.929	17.840	0.312	18.539	0.285	18.747
0.423	17.521	0.312	17.687	0.938	17.843	0.319	18.542	0.290	18.750
0.405	17.524	0.310	17.690	0.938	17.845	0.336	18.545	0.273	18.753
0.431	17.526	0.313	17.692	0.929	17.848	0.352	18.548	0.285	18.756
0.426	17.531	0.302	17.695	0.929	17.851	0.344	18.554	0.268	18.758
0.436	17.533	0.291	17.698	0.897	17.853	0.360	18.558	0.280	18.762
0.462	17.536	0.288	17.700	0.868	17.856	0.359	18.561	0.270	18.764
0.453	17.540	0.286	17.704	0.794	17.859	0.365	18.565	0.280	18.766
0.469	17.542	0.294	17.706	0.770	17.862	0.372	18.568	0.280	18.770
0.487	17.545	0.282	17.709	0.748	17.864	0.365	18.571	0.280	18.773
0.492	17.552	0.302	17.712	0.704	17.867	0.374	18.574	0.754	21.509
0.506	17.555	0.295	17.714	0.674	17.870	0.384	18.577	0.756	21.510
0.505	17.557	0.295	17.717	0.637	17.872	0.406	18.581	0.812	21.513
0.502	17.561	0.294	17.720	0.612	17.876	0.392	18.583	0.867	21.516
0.516	17.564	0.289	17.723	0.563	17.878	0.410	18.586	0.935	21.522
0.489	17.566	0.283	17.725	0.547	17.880	0.417	18.590	0.935	21.524
0.514	17.570	0.304	17.728	0.512	17.884	0.433	18.593	0.951	21.530
0.510	17.572	0.289	17.731	0.488	17.886	0.439	18.595	0.939	21.533
0.504	17.575	0.303	17.733	0.471	17.889	0.449	18.601	0.925	21.536
0.508	17.578	0.315	17.736	0.433	17.892	0.469	18.604	0.940	21.542
0.509	17.581	0.310	17.739	0.421	17.894	0.461	18.608	0.924	21.547
0.497	17.583	0.323	17.741	0.416	17.897	0.475	18.613	0.905	21.550
0.519	17.586	0.327	17.744	0.396	17.900	0.489	18.618	0.893	21.553
0.511	17.589	0.326	17.747	0.390	17.903	0.487	18.625	0.846	21.556
0.504	17.591	0.335	17.749	0.381	17.905	0.477	18.629	0.807	21.559
0.493	17.594	0.340	17.753	0.362	17.908	0.489	18.632	0.772	21.562
0.476	17.597	0.351	17.755	0.344	17.911	0.475	18.636	0.721	21.565
0.483	17.599	0.347	17.758	0.338	17.913	0.481	18.640	0.677	21.568
0.491	17.603	0.356	17.761	0.347	17.916	0.481	18.643	0.648	21.571
0.465	17.605	0.372	17.764	0.328	17.919	0.460	18.650	0.607	21.573
0.469	17.607	0.372	17.766	0.327	17.921	0.454	18.653	0.588	21.576
0.456	17.611	0.381	17.769	0.323	17.925	0.452	18.656	0.580	21.579
0.449	17.613	0.393	17.772	0.320	17.927	0.446	18.664	0.311	21.634
0.447	17.616	0.401	17.774	0.322	17.930	0.434	18.667	0.311	21.636
0.419	17.619	0.412	17.778	0.327	17.933	0.449	18.670	0.297	21.639
0.420	17.621	0.421	17.780	0.301	17.935	0.418	18.674	0.310	21.642
0.411	17.624	0.447	17.782	0.315	17.938	0.418	18.677	0.289	21.647
0.421	17.627	0.475	17.786	0.290	17.941	0.389	18.680	0.307	21.653
0.405	17.629	0.496	17.788	0.284	17.943	0.388	18.685	0.293	21.655
0.399	17.632	0.507	17.790	0.305	17.946	0.386	18.688	0.268	21.658
0.384	17.636	0.542	17.794	0.274	17.949	0.368	18.691	0.271	21.661
0.379	17.638	0.556	17.796	0.280	17.952	0.359	18.695	0.290	21.664
0.373	17.641	0.598	17.799	0.280	17.954	0.355	18.698	0.275	21.666
0.372	17.644	0.620	17.802	0.261	17.958	0.360	18.701	0.284	21.672
0.374	17.646	0.654	17.804	0.271	17.960	0.331	18.706	0.314	21.674
0.349	17.649	0.688	17.807	0.267	17.962	0.345	18.709	0.302	21.680
0.355	17.653	0.743	17.810	0.285	18.497	0.339	18.712	0.280	21.683
0.355	17.656	0.774	17.813	0.280	18.503	0.328	18.716	0.209	21.685
0.351	17.658	0.817	17.815	0.299	18.507	0.324	18.719	0.331	21.694
0.335	17.661	0.848	17.818	0.283	18.510	0.313	18.722	0.310	21.696
0.328	17.664	0.887	17.821	0.290	18.513	0.324	18.726	0.302	21.699
0.337	17.666	0.904	17.823	0.317	18.519	0.304	18.729	0.321	21.702
0.344	17.671	0.926	17.827	0.307	18.522	0.284	18.732	0.321	21.704
0.327	17.674	0.919	17.829	0.298	18.525	0.308	18.736	0.280	21.707

Table continued on next page

Table 2. V616 Cam observations, ΔV, ΔR_c, and ΔI_c, variable star minus comparison star, cont.

ΔI	HJD 2457800+	ΔI	HJD 2457800+	ΔI	HJD 2457800+	ΔI	HJD 2457800+	ΔI	HJD 2457800+
0.426	17.507	0.383	17.676	0.966	17.832	0.371	18.529	0.333	18.736
0.417	17.511	0.370	17.680	0.960	17.835	0.375	18.532	0.340	18.739
0.420	17.513	0.366	17.682	0.964	17.837	0.365	18.534	0.331	18.741
0.436	17.515	0.353	17.684	0.970	17.840	0.356	18.539	0.327	18.745
0.466	17.522	0.353	17.688	0.970	17.843	0.374	18.542	0.323	18.748
0.455	17.524	0.367	17.690	0.958	17.846	0.386	18.545	0.335	18.750
0.471	17.526	0.364	17.692	0.971	17.848	0.365	18.549	0.319	18.754
0.482	17.531	0.363	17.692	0.914	17.851	0.346	18.551	0.328	18.756
0.510	17.533	0.341	17.696	0.933	17.854	0.407	18.554	0.326	18.758
0.496	17.536	0.351	17.701	0.893	17.856	0.397	18.559	0.312	18.762
0.524	17.540	0.344	17.704	0.851	17.859	0.454	18.561	0.324	18.764
0.553	17.542	0.351	17.707	0.859	17.862	0.408	18.565	0.321	18.767
0.555	17.545	0.349	17.709	0.803	17.864	0.403	18.568	0.333	18.771
0.556	17.552	0.343	17.712	0.736	17.868	0.419	18.572	0.323	18.774
0.570	17.555	0.344	17.715	0.700	17.870	0.426	18.575	0.799	21.509
0.580	17.557	0.336	17.717	0.689	17.873	0.430	18.577	0.861	21.513
0.587	17.562	0.356	17.720	0.653	17.876	0.435	18.581	0.842	21.516
0.582	17.564	0.363	17.723	0.619	17.878	0.451	18.584	0.888	21.519
0.570	17.567	0.360	17.725	0.625	17.881	0.445	18.587	0.968	21.525
0.588	17.570	0.349	17.729	0.580	17.884	0.466	18.590	0.974	21.528
0.581	17.573	0.371	17.731	0.548	17.886	0.478	18.593	0.969	21.531
0.562	17.575	0.364	17.733	0.525	17.889	0.484	18.596	0.999	21.542
0.569	17.578	0.386	17.737	0.494	17.892	0.522	18.601	0.986	21.545
0.581	17.581	0.366	17.739	0.491	17.895	0.562	18.605	0.964	21.551
0.569	17.583	0.378	17.741	0.446	17.897	0.539	18.608	0.943	21.554
0.573	17.587	0.384	17.745	0.449	17.900	0.557	18.614	0.884	21.556
0.583	17.589	0.383	17.747	0.446	17.903	0.541	18.619	0.854	21.559
0.579	17.591	0.383	17.750	0.434	17.905	0.547	18.626	0.801	21.562
0.582	17.595	0.397	17.753	0.431	17.909	0.541	18.629	0.711	21.568
0.559	17.597	0.404	17.756	0.421	17.911	0.538	18.632	0.679	21.571
0.539	17.600	0.406	17.758	0.420	17.913	0.528	18.637	0.651	21.574
0.522	17.603	0.423	17.761	0.434	17.917	0.566	18.640	0.640	21.577
0.531	17.605	0.425	17.764	0.406	17.919	0.537	18.643	0.622	21.579
0.509	17.608	0.424	17.766	0.410	17.922	0.531	18.650	0.586	21.582
0.507	17.611	0.431	17.770	0.369	17.925	0.520	18.654	0.344	21.634
0.500	17.613	0.455	17.772	0.388	17.927	0.506	18.657	0.360	21.637
0.502	17.616	0.465	17.775	0.383	17.930	0.483	18.664	0.347	21.645
0.479	17.619	0.471	17.778	0.375	17.933	0.488	18.667	0.334	21.648
0.470	17.622	0.497	17.780	0.376	17.935	0.479	18.670	0.319	21.650
0.467	17.624	0.504	17.783	0.355	17.938	0.469	18.674	0.336	21.656
0.457	17.627	0.533	17.786	0.353	17.941	0.456	18.677	0.299	21.658
0.452	17.630	0.541	17.788	0.338	17.944	0.433	18.680	0.325	21.661
0.437	17.632	0.577	17.791	0.352	17.946	0.440	18.686	0.337	21.664
0.430	17.636	0.597	17.794	0.347	17.949	0.424	18.689	0.333	21.667
0.410	17.638	0.608	17.796	0.354	17.952	0.430	18.691	0.320	21.669
0.410	17.641	0.634	17.799	0.327	17.954	0.404	18.696	0.346	21.675
0.405	17.644	0.680	17.802	0.337	17.958	0.407	18.699	0.339	21.678
0.416	17.646	0.705	17.805	0.340	17.960	0.390	18.702	0.327	21.680
0.389	17.649	0.737	17.807	0.357	17.963	0.377	18.707	0.333	21.683
0.410	17.653	0.782	17.811	0.355	18.497	0.382	18.710	0.341	21.694
0.400	17.656	0.824	17.813	0.350	18.500	0.381	18.713	0.321	21.699
0.403	17.658	0.847	17.816	0.354	18.507	0.371	18.717	0.360	21.702
0.387	17.662	0.900	17.819	0.335	18.510	0.367	18.720	0.368	21.705
0.368	17.664	0.938	17.821	0.344	18.513	0.355	18.723	0.406	21.718
0.371	17.666	0.918	17.824	0.352	18.519	0.365	18.727	0.401	21.721
0.366	17.671	0.941	17.827	0.347	18.522	0.342	18.729	0.395	21.724
0.372	17.674	0.970	17.829	0.359	18.525	0.344	18.732	0.416	21.727

Table 3. O–C residual calculations of V616 Cam.

	Cycle	*Epochs 2400000.0+*	*Error*	*Linear Residuals*	*Quadratic Residuals*	*Weight*	*Reference*
1	–12108.5	51419.9562	—	–0.0280	–0.0002	1.0	Shaw (1990, 1994)
2	–12108.0	51420.2204	—	–0.0281	–0.0002	0.5	VSX (Watson *et al.* 2014)
3	–4238.5	55578.3813	0.0210	0.0600	0.0009	1.0	Hubscher and Lehmann (2012)
4	–4238	55578.6463	0.0041	0.0608	0.0017	1.0	Hubscher and Lehmann (2012)
5	–828.5	57380.0848	0.0027	–0.0064	–0.0119	0.5	This work; NSVS (Wozniak *et al.* 2004)
6	–770.0	57410.9985	0.0003	–0.0028	–0.0069	0.5	This work; NSVS (Wozniak *et al.* 2004)
7	–0.5	57817.5742	0.0013	–0.0142	0.0017	1.0	This work
8	0.0	57817.8376	0.0001	–0.0150	0.0009	1.0	This work
9	1.5	57818.6310	0.0002	–0.0142	0.0018	1.0	This work
10	7.0	57821.5364	0.0004	–0.0149	0.0013	1.0	This work
11	47.0	57842.6710	0.0002	–0.0158	0.0015	1.0	This work

Table 4. Light curve characteristics for V616 Cam.

Filter	*Phase 0.25*	*Magnitude Min. I*	*± σ*	*Phase 0.75*	*Magnitude Max. I*	*± σ*
V		0.886	± 0.011		0.193	± 0.014
R_c		0.935	± 0.007		0.275	± 0.009
I_c		0.971	± 0.011		0.335	± 0.018

Filter	*Phase 0.5*	*Magnitude Min. II*	*± σ*	*Phase 0.0*	*Magnitude Max. II*	*± σ*
V		0.428	± 0.009		0.283	± 0.010
R_c		0.497	± 0.014		0.385	± 0.005
I_c		0.563	± 0.020		0.335	± 0.014

Filter	*Min. I – Max. I*	*± σ*	*Max. II – Max. I*	*± σ*	*Min. I – Min. II*	*± σ*
V	0.693	± 0.025	0.090	± 0.024	0.458	± 0.020
R_c	0.660	± 0.016	0.090	± 0.014	0.439	± 0.022
I_c	0.636	± 0.029	0.000	± 0.032	0.408	± 0.031

Filter	*Max. II – Max. I*	*± σ*	*Min. II – Max. I*	*± σ*
V	0.090	± 0.024	0.235	± 0.023
R_c	0.109	± 0.014	0.221	± 0.023
I_c	0.000	± 0.0325	0.227	± 0.038

Table 5a. VR_cI_c synthetic curve solution input parameters for V616 Cam.

Parameters	*Values*
λ_V, λ_R, λ_I (nm)	550, 640, 790
$x_{bol1,2}$, $y_{bol1,2}$ (bolometric limb darkening)	0.638, 0.637, 0.248, 0.148
$x_{1I,2I}$, $y_{1I,2I}$ (limb darkening)	0.539, 0.656, 0.281, 0.160
$x_{1R,2}R$, $y_{1R,2R}$ (limb darkening)	0.624, 0.744, 0.291, 0.128
$x_{1V,2V}$, $y_{1V,2V}$ (limb darkening)	0.698, 0.799, 0.282, 0.054
g_1 , g_2 (gravity darkening)	0.32
A_1 , A_2 (albedo)	0.5

Table 5b. V,R_c,I_c Wilson-Devinney program solution parameters.

Parameters	*Mode 2 Detached Solution*	*Mode 4 Semi-detached (V1010 Oph)*	*Mode 5 Semi-detached (Algol)*
Inclination (°)	85.0 ± 0.2	86.75 ± 0.23	86.75 ± 0.30
T_1, T_2 (K)	6750*, 4662 ± 5	6750*, 4703 ± 6	6750*, 4734 ± 6
Ω_1 potential	2.5857 ± 0.0022	2.5889	2.583 ± 0.002,
Ω_2 potential	2.5871 ± 0.0021	2.602 ± 0.002	2.572
q (m_2 / m_1)	0.3554 ± 0.0006	0.3572 ± 0.0006	0.3489 ± 0.0012
Fill-outs: F_1 (%),	99.99	100	99.6
F_2 (%)	99.78	99.5	100
$L_1/(L_1+L_2)_I$	0.9076 ± 0.0007	0.9060 ± 0.0007	0.9021 ± 0.0007
$L_1/(L_1+L_2)_R$	0.9259 ± 0.0010	0.9242 ± 0.0010	0.9205 ± 0.0010
$L_1/(L_1+L_2)_V$	0.9451 ± 0.0006	0.9432 ± 0.0006	0.9399 ± 0.0006
JDo (days)	2457817.8373 ± 0.0001	2457817.8373 ± .0001	2457817.8373 ± 0.0001
Period (days)	0.52847 ± 0.00003	0. 528468 ± 0.00003	0.528466 ± 0.000035
r_1, r_2 (pole)	0.442 ± 0.001, 0.273 ± 0.004	0.4419 ± 0.0009, 0.2715 ± 0.0035	0.4417 ± 0.0009,0.2723 ± 0.0005
r_1, r_2 (point)	0.6 ± 0.1, 0.38 ± 0.08	— , 0.3626 ± 0.0265	0.574 ± 0.010, —
r_1, r_2 (side)	0.473 ± 0.002, 0.285 ± 0.004	0.473 ± 0.001, 0.283 ± 0.004	0.472 ± 0.001,0.2836 ± 0.0006
r_1, r_2 (back)	0.4995 ± 0.0025, 0.317 ± 0.007	0.499 ± 0.001,0.313 ± 0.007	0.498 ± 0.002,0.3164 ± 0.0006
Spot Parameters	Star 1, Cool Spot		
Colatitude (°)	110 ± 5.	107 ± 2	107 ± 4
Longitude (°)	134.5 ± 3.4	128.5 ± 3.1	135 ± 1
Spot radius (°)	18.4 ± 0.8	14.0 ± 0.4	14.7 ± 0.5
Tfact	0.959 ± 0.003	0.940 ± 0.004	0.940 ± 0.004
$\Sigma(res)^2$	0.262956	0.265574	0.270075

**The 6750 K primary temperature carries a ±400 K uncertainty.*